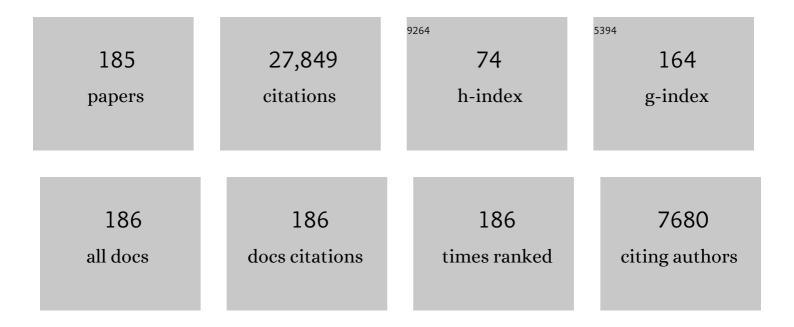
List of Publications by Year in descending order

Source: https://exaly.com/author-pdf/11777303/publications.pdf Version: 2024-02-01



SHAN CAO

#	Article	IF	CITATIONS
1	In situ analysis of major and trace elements of anhydrous minerals by LA-ICP-MS without applying an internal standard. Chemical Geology, 2008, 257, 34-43.	3.3	3,342
2	Recycling lower continental crust in the North China craton. Nature, 2004, 432, 892-897.	27.8	1,523
3	Reappraisement and refinement of zircon U-Pb isotope and trace element analyses by LA-ICP-MS. Science Bulletin, 2010, 55, 1535-1546.	1.7	1,347
4	Accurate U-Pb Age and Trace Element Determinations of Zircon by Laser Ablation-Inductively Coupled Plasma-Mass Spectrometry. Geostandards and Geoanalytical Research, 2004, 28, 353-370.	1.9	1,191
5	Improved in situ Hf isotope ratio analysis of zircon using newly designed X skimmer cone and jet sample cone in combination with the addition of nitrogen by laser ablation multiple collector ICP-MS. Journal of Analytical Atomic Spectrometry, 2012, 27, 1391.	3.0	857
6	Simultaneous determinations of U–Pb age, Hf isotopes and trace element compositions of zircon by excimer laser-ablation quadrupole and multiple-collector ICP-MS. Chemical Geology, 2008, 247, 100-118.	3.3	829
7	Chemical composition of the continental crust as revealed by studies in East China. Geochimica Et Cosmochimica Acta, 1998, 62, 1959-1975.	3.9	813
8	Re–Os evidence for replacement of ancient mantle lithosphere beneath the North China craton. Earth and Planetary Science Letters, 2002, 198, 307-322.	4.4	802
9	First evidence of >3.2 Ga continental crust in the Yangtze craton of south China and its implications for Archean crustal evolution and Phanerozoic tectonics. Geology, 2000, 28, 11.	4.4	707
10	Contrasting geochemical and Sm-Nd isotopic compositions of Archean metasediments from the Kongling high-grade terrain of the Yangtze craton: evidence for cratonic evolution and redistribution of REE during crustal anatexis. Geochimica Et Cosmochimica Acta, 1999, 63, 2071-2088.	3.9	585
11	Petrology and geochemistry of spinel peridotite xenoliths from Hannuoba and Qixia, North China craton. Lithos, 2004, 77, 609-637.	1.4	505
12	Geochemistry and magmatic history of eclogites and ultramafic rocks from the Chinese continental scientific drill hole: Subduction and ultrahigh-pressure metamorphism of lower crustal cumulates. Chemical Geology, 2008, 247, 133-153.	3.3	504
13	Signal enhancement in laser ablation ICP-MS by addition of nitrogen in the central channel gas. Journal of Analytical Atomic Spectrometry, 2008, 23, 1093.	3.0	494
14	Upper crustal abundances of trace elements: A revision and update. Chemical Geology, 2008, 253, 205-221.	3.3	482
15	Determination of Forty Two Major and Trace Elements in USGS and NIST SRM Glasses by Laser Ablation-Inductively Coupled Plasma-Mass Spectrometry. Geostandards and Geoanalytical Research, 2002, 26, 181-196.	3.1	454
16	Geochronology of the Mesozoic volcanic rocks in the Great Xing'an Range, northeastern China: Implications for subduction-induced delamination. Chemical Geology, 2010, 276, 144-165.	3.3	419
17	"Wave―Signal-Smoothing and Mercury-Removing Device for Laser Ablation Quadrupole and Multiple Collector ICPMS Analysis: Application to Lead Isotope Analysis. Analytical Chemistry, 2015, 87, 1152-1157.	6.5	415
18	Recycling deep cratonic lithosphere and generation of intraplate magmatism in the North China Craton. Earth and Planetary Science Letters, 2008, 270, 41-53.	4.4	412

#	Article	IF	CITATIONS
19	Zircon U-Pb age and Hf-O isotope evidence for Paleoproterozoic metamorphic event in South China. Precambrian Research, 2006, 151, 265-288.	2.7	359
20	Zircon isotope evidence for ≥3.5Ga continental crust in the Yangtze craton of China. Precambrian Research, 2006, 146, 16-34.	2.7	348
21	Zircon U–Pb age and Hf isotope evidence for 3.8ÂGa crustal remnant and episodic reworking of Archean crust in South China. Earth and Planetary Science Letters, 2006, 252, 56-71.	4.4	345
22	Constraints on timing of peak and retrograde metamorphism in the Dabie Shan Ultrahigh-Pressure Metamorphic Belt, east-central China, using U–Th–Pb dating of zircon and monazite. Chemical Geology, 2002, 186, 315-331.	3.3	256
23	How mafic is the lower continental crust?. Earth and Planetary Science Letters, 1998, 161, 101-117.	4.4	247
24	3.45 Ga granitic gneisses from the Yangtze Craton, South China: Implications for Early Archean crustal growth. Precambrian Research, 2014, 242, 82-95.	2.7	245
25	Zircon U–Pb age and trace element evidence for Paleoproterozoic granulite-facies metamorphism and Archean crustal rocks in the Dabie Orogen. Lithos, 2008, 101, 308-322.	1.4	240
26	U–Pb zircon ages and Nd, Sr, and Pb isotopes of lower crustal xenoliths from North China Craton: insights on evolution of lower continental crust. Chemical Geology, 2004, 211, 87-109.	3.3	228
27	Recycled crust controls contrasting source compositions of Mesozoic and Cenozoic basalts in the North China Craton. Geochimica Et Cosmochimica Acta, 2008, 72, 2349-2376.	3.9	223
28	Heterogeneous magnesium isotopic composition of the upper continental crust. Geochimica Et Cosmochimica Acta, 2010, 74, 6867-6884.	3.9	210
29	Simultaneous in-situ determination of U-Pb age and trace elements in zircon by LA-ICP-MS in 20 μm spot size. Science Bulletin, 2007, 52, 1257-1264.	1.7	209
30	Interaction of adakitic melt-peridotite: Implications for the high-Mg# signature of Mesozoic adakitic rocks in the eastern North China Craton. Earth and Planetary Science Letters, 2008, 265, 123-137.	4.4	207
31	Geochemical and Sr–Nd–Pb isotopic compositions of Cretaceous granitoids: constraints on tectonic framework and crustal structure of the Dabieshan ultrahigh-pressure metamorphic belt, China. Chemical Geology, 2002, 186, 281-299.	3.3	205
32	A "wire―signal smoothing device for laser ablation inductively coupled plasma mass spectrometry analysis. Spectrochimica Acta, Part B: Atomic Spectroscopy, 2012, 78, 50-57.	2.9	205
33	A-type granite and adakitic magmatism association in Songpan–Garze fold belt, eastern Tibetan Plateau: Implication for lithospheric delamination. Lithos, 2007, 97, 323-335.	1.4	189
34	Mesozoic crustal thickening of the eastern North China craton: Evidence from eclogite xenoliths and petrologic implications. Geology, 2006, 34, 721.	4.4	186
35	Geochemistry and zircon U–Pb geochronology of Paleoproterozoic arc related granitoid in the Northwestern Yangtze Block and its geological implications. Precambrian Research, 2012, 200-203, 26-37.	2.7	179
36	Geochemistry of lower crustal xenoliths from Neogene Hannuoba basalt, North China craton: implications for petrogenesis and lower crustal composition. Geochimica Et Cosmochimica Acta, 2001, 65, 2589-2604.	3.9	173

#	Article	IF	CITATIONS
37	Episodic crustal growth of North China as revealed by U–Pb age and Hf isotopes of detrital zircons from modern rivers. Geochimica Et Cosmochimica Acta, 2009, 73, 2660-2673.	3.9	169
38	Diffusion-driven magnesium and iron isotope fractionation in Hawaiian olivine. Earth and Planetary Science Letters, 2011, 308, 317-324.	4.4	169
39	Geochemistry, zircon U–Pb age and Hf isotope compositions of Paleoproterozoic aluminous A-type granites from the Kongling terrain, Yangtze Block: Constraints on petrogenesis and geologic implications. Condwana Research, 2012, 22, 140-151.	6.0	169
40	2.6–2.7 Ga crustal growth in Yangtze craton, South China. Precambrian Research, 2013, 224, 472-490.	2.7	162
41	Changes in marine productivity and redox conditions during the Late Ordovician Hirnantian glaciation. Palaeogeography, Palaeoclimatology, Palaeoecology, 2015, 420, 223-234.	2.3	157
42	Age and nature of eclogites in the Huwan shear zone, and the multi-stage evolution of the Qinling-Dabie-Sulu orogen, central China. Earth and Planetary Science Letters, 2009, 277, 345-354.	4.4	146
43	Petrogenesis of Neoarchean TTG rocks in the Yangtze Craton and its implication for the formation of Archean TTGs. Precambrian Research, 2014, 254, 73-86.	2.7	141
44	Geochemical, age, and isotopic constraints on the location of the Sino–Korean/Yangtze Suture and evolution of the Northern Dabie Complex, east central China. Bulletin of the Geological Society of America, 2004, 116, 698.	3.3	139
45	Accurate determinations of fifty-four major and trace elements in carbonate by LA–ICP-MS using normalization strategy of bulk components as 100%. Chemical Geology, 2011, 284, 283-295.	3.3	138
46	Volatile organic solvent-induced signal enhancements in inductively coupled plasma-mass spectrometry: a case study of methanol and acetone. Spectrochimica Acta, Part B: Atomic Spectroscopy, 2004, 59, 1463-1470.	2.9	131
47	Petrophysical studies on rocks from the Dabie ultrahigh-pressure (UHP) metamorphic belt, Central China: implications for the composition and delamination of the lower crust. Tectonophysics, 1999, 301, 191-215.	2.2	127
48	U–Pb zircon age, geochemical and Sr–Nd–Pb–Hf isotopic constraints on age and origin of alkaline intrusions and associated mafic dikes from Sulu orogenic belt, Eastern China. Lithos, 2008, 106, 365-379.	1.4	127
49	Delamination and destruction of the North China Craton. Science Bulletin, 2009, 54, 3367-3378.	9.0	126
50	In situ sulfur isotopes (δ 34 S and δ 33 S) analyses in sulfides and elemental sulfur using high sensitivity cones combined with the addition of nitrogen by laser ablation MC-ICP-MS. Analytica Chimica Acta, 2016, 911, 14-26.	5.4	126
51	Episodic Paleoarchean-Paleoproterozoic (3.3–2.0 Ga) granitoid magmatism in Yangtze Craton, South China: Implications for late Archean tectonics. Precambrian Research, 2015, 270, 246-266.	2.7	125
52	Silurian-Devonian provenance changes of South Qinling basins: implications for accretion of the Yangtze (South China) to the North China cratons. Tectonophysics, 1995, 250, 183-197.	2.2	123
53	Contrasting matrix induced elemental fractionation in NIST SRM and rock glasses during laser ablation ICP-MS analysis at high spatial resolution. Journal of Analytical Atomic Spectrometry, 2011, 26, 425-430.	3.0	123
54	Mapping lithospheric boundaries using Os isotopes of mantle xenoliths: An example from the North China Craton. Geochimica Et Cosmochimica Acta, 2011, 75, 3881-3902.	3.9	118

#	Article	IF	CITATIONS
55	Petrogenesis of Late Mesozoic mafic dykes in the Jiaodong Peninsula, eastern North China Craton and implications for the foundering of lower crust. Lithos, 2009, 113, 621-639.	1.4	117
56	Zircon U–Pb and trace element data from rocks of the Huai'an Complex: New insights into the late Paleoproterozoic collision between the Eastern and Western Blocks of the North China Craton. Precambrian Research, 2010, 178, 59-71.	2.7	112
57	Destruction of the North China Craton: Delamination or thermal/chemical erosion? Mineral chemistry and oxygen isotope insights from websterite xenoliths. Gondwana Research, 2013, 23, 119-129.	6.0	112
58	A local aerosol extraction strategy for the determination of the aerosol composition in laser ablation inductively coupled plasma mass spectrometry. Journal of Analytical Atomic Spectrometry, 2008, 23, 1192.	3.0	111
59	Zircon U–Pb geochronology and major, trace elemental and Sr–Nd–Pb isotopic geochemistry of mafic dykes in western Shandong Province, east China: Constrains on their petrogenesis and geodynamic significance. Chemical Geology, 2008, 255, 329-345.	3.3	109
60	Rare-earth element patterns in conodont albid crowns: Evidence for massive inputs of volcanic ash during the latest Permian biocrisis?. Global and Planetary Change, 2013, 105, 135-151.	3.5	107
61	Zircon U–Pb age and Sr–Nd–Hf isotope geochemistry of Permian granodiorite and associated gabbro in the Songliao Block, NE China and implications for growth of juvenile crust. Lithos, 2010, 114, 423-436.	1.4	101
62	Continental origin of eclogites in the North Qinling terrane and its tectonic implications. Precambrian Research, 2013, 230, 13-30.	2.7	101
63	Accurate Determination of Sr Isotopic Compositions in Clinopyroxene and Silicate Glasses by <scp>LA</scp> â€ <scp>MC</scp> â€ <scp>ICP</scp> â€ <scp>MS</scp> . Geostandards and Geoanalytical Research, 2016, 40, 85-99.	3.1	100
64	Lithium isotopic composition and concentration of the deep continental crust. Chemical Geology, 2008, 255, 47-59.	3.3	98
65	Compositional evolution of the upper continental crust through time, as constrained by ancient glacial diamictites. Geochimica Et Cosmochimica Acta, 2016, 186, 316-343.	3.9	98
66	Timing of UHP metamorphism in the Hong'an area, western Dabie Mountains, China: evidence from zircon U–Pb age, trace element and Hf isotope composition. Contributions To Mineralogy and Petrology, 2007, 155, 123-133.	3.1	95
67	Pb isotopes of granitoids suggest Devonian accretion of Yangtze (South China) craton to North China craton. Geology, 1997, 25, 1015.	4.4	91
68	Zircon U–Pb age, geochemistry and Sr–Nd–Pb isotopic compositions of adakitic volcanic rocks from Jiaodong, Shandong Province, Eastern China: Constraints on petrogenesis and implications. Journal of Asian Earth Sciences, 2009, 35, 445-458.	2.3	88
69	Geochemistry of peridotite xenoliths in Early Cretaceous high-Mg# diorites from the Central Orogenic Block of the North China Craton: The nature of Mesozoic lithospheric mantle and constraints on lithospheric thinning. Chemical Geology, 2010, 270, 257-273.	3.3	87
70	The 2.65 Ga A-type granite in the northeastern Yangtze craton: Petrogenesis and geological implications. Precambrian Research, 2015, 258, 247-259.	2.7	87
71	Melting-induced fluid flow during exhumation of gneisses of the Sulu ultrahigh-pressure terrane. Lithos, 2010, 120, 490-510.	1.4	85
72	In situ U–Pb dating and trace element analysis of zircons in thin sections of eclogite: Refining constraints on the ultra high-pressure metamorphism of the Sulu terrane, China. Chemical Geology, 2010, 269, 237-251.	3.3	84

#	Article	IF	CITATIONS
73	Applications of LA-ICP-MS in the elemental analyses of geological samples. Science Bulletin, 2013, 58, 3863-3878.	1.7	81
74	U-Pb age, trace-element, and Hf-isotope compositions of zircon in a quartz vein from eclogite in the western Dabie Mountains: Constraints on fluid flow during early exhumation of ultrahigh-pressure rocks. American Mineralogist, 2009, 94, 303-312.	1.9	78
75	Total Rock Dissolution Using Ammonium Bifluoride (NH ₄ HF ₂) in Screw-Top Teflon Vials: A New Development in Open-Vessel Digestion. Analytical Chemistry, 2012, 84, 10686-10693.	6.5	77
76	Geochronological and geochemical constraints on the petrogenesis of alkaline ultramafic dykes from southwest Guizhou Province, SW China. Lithos, 2010, 114, 253-264.	1.4	75
77	Processes controlling highly siderophile element fractionations in xenolithic peridotites and their influence on Os isotopes. Earth and Planetary Science Letters, 2010, 297, 287-297.	4.4	75
78	Platinum group element abundances in the upper continental crust revisited – New constraints from analyses of Chinese loess. Geochimica Et Cosmochimica Acta, 2012, 93, 63-76.	3.9	73
79	Physical properties of ultrahigh-pressure metamorphic rocks from the Sulu terrain, eastern central China: implications for the seismic structure at the Donghai (CCSD) drilling site. Tectonophysics, 2002, 354, 315-330.	2.2	72
80	Seismic properties and densities of middle and lower crustal rocks exposed along the North China Geoscience Transect. Earth and Planetary Science Letters, 1996, 139, 439-455.	4.4	69
81	In situ Nd isotope analyses in geological materials with signal enhancement and non-linear mass dependent fractionation reduction using laser ablation MC-ICP-MS. Journal of Analytical Atomic Spectrometry, 2015, 30, 232-244.	3.0	69
82	Deep subduction of continental crust in accretionary orogen: Evidence from U–Pb dating on diamond-bearing zircons from the Qinling orogen, central China. Lithos, 2014, 190-191, 420-429.	1.4	68
83	Age and geochemistry of Silurian gabbroic rocks in the Tongbai orogen, central China: Implications for the geodynamic evolution of the North Qinling arc–back-arc system. Lithos, 2013, 179, 1-15.	1.4	64
84	Genesis of adakitic granitoids by partial melting of thickened lower crust and its implications for early crustal growth: A case study from the Huichizi pluton, Qinling orogen, central China. Lithos, 2015, 238, 1-12.	1.4	64
85	Geochemistry of eclogite xenoliths in Mesozoic adakitic rocks from Xuzhou-Suzhou area in central China and their tectonic implications. Lithos, 2009, 107, 269-280.	1.4	63
86	Accurate determination of lithium isotope ratios by MC-ICP-MS without strict matrix-matching by using a novel washing method. Journal of Analytical Atomic Spectrometry, 2016, 31, 390-397.	3.0	63
87	In-situ trace elements and Li and Sr isotopes in peridotite xenoliths from Kuandian, North China Craton: Insights into Pacific slab subduction-related mantle modification. Chemical Geology, 2013, 354, 107-123.	3.3	62
88	Recycling of sediment into the mantle source of K-rich mafic rocks: Sr–Nd–Hf–O isotopic evidence from the Fushui complex in the Qinling orogen. Contributions To Mineralogy and Petrology, 2014, 168, 1.	3.1	62
89	Platinum-group element abundances and Re–Os isotopic systematics of the upper continental crust through time: Evidence from glacial diamictites. Geochimica Et Cosmochimica Acta, 2016, 191, 1-16.	3.9	61
90	Silurian granulite-facies metamorphism, and coeval magmatism and crustal growth in the Tongbai orogen, central China. Lithos, 2011, 125, 249-271.	1.4	60

#	Article	lF	CITATIONS
91	Single zircon U-Pb dating of the Kongling high-grade metamorphic terrain: Evidence for >3.2 Ga old continental crust in the Yangtze craton. Science in China Series D: Earth Sciences, 2001, 44, 326-335.	0.9	59
92	Onset of oxidative weathering of continents recorded in the geochemistry of ancient glacial diamictites. Earth and Planetary Science Letters, 2014, 408, 87-99.	4.4	59
93	First direct evidence of sedimentary carbonate recycling in subduction-related xenoliths. Scientific Reports, 2015, 5, 11547.	3.3	57
94	Calcium Isotopic Compositions of Sixteen <scp>USGS</scp> Reference Materials. Geostandards and Geoanalytical Research, 2017, 41, 93-106.	3.1	55
95	Mesozoic–Cenozoic mantle evolution beneath the North China Craton: A new perspective from Hf–Nd isotopes of basalts. Gondwana Research, 2015, 27, 1574-1585.	6.0	54
96	The recognizing of ca. 1.95 Ga tectono-thermal eventin Kongling nucleus and its significance for the evolution of Yangtze Block, South China. Science Bulletin, 2001, 46, 326-329.	1.7	52
97	Record of multiple stage channelized fluid and melt activities in deeply subducted slab from zircon U–Pb age and Hf–O isotope compositions. Geochimica Et Cosmochimica Acta, 2014, 144, 1-24.	3.9	51
98	Continental growth through accreted oceanic arc: Zircon Hf–O isotope evidence for granitoids from the Qinling orogen. Geochimica Et Cosmochimica Acta, 2016, 182, 109-130.	3.9	51
99	Eclogite-melt/peridotite reaction: Experimental constrains on the destruction mechanism of the North China Craton. Science China Earth Sciences, 2010, 53, 797-809.	5.2	50
100	Re–Os evidence for the age and origin of peridotites from the Dabie–Sulu ultrahigh pressure metamorphic belt, China. Chemical Geology, 2007, 236, 323-338.	3.3	49
101	Measured and calculated seismic velocities and densities for granulites from xenolith occurrences and adjacent exposed lower crustal sections: A comparative study from the North China craton. Journal of Geophysical Research, 2000, 105, 18965-18976.	3.3	48
102	Geochronology, geochemistry, and isotope compositions of Piaochi S-type granitic intrusion in the Qinling orogen, central China: Petrogenesis and tectonic significance. Lithos, 2014, 202-203, 347-362.	1.4	47
103	Suppression of interferences for direct determination of arsenic in geological samples by inductively coupled plasma mass spectrometry. Journal of Analytical Atomic Spectrometry, 2005, 20, 1263.	3.0	46
104	NH4F assisted high pressure digestion of geological samples for multi-element analysis by ICP-MS. Journal of Analytical Atomic Spectrometry, 2010, 25, 408.	3.0	44
105	The uncertainty budget of the multi-element analysis of glasses using LA-ICP-MS. Journal of Analytical Atomic Spectrometry, 2007, 22, 122-130.	3.0	43
106	Magnesium isotopic composition of the deep continental crust. American Mineralogist, 2016, 101, 243-252.	1.9	42
107	Reassessment of HF/HNO3 Decomposition Capability in the High-Pressure Digestion of Felsic Rocks for Multi-Element Determination by ICP-MS. Geostandards and Geoanalytical Research, 2012, 36, 271-289.	3.1	41
108	Rapid bulk rock decomposition by ammonium fluoride (NH4F) in open vessels at an elevated digestion temperature. Chemical Geology, 2013, 355, 144-152.	3.3	41

#	Article	IF	CITATIONS
109	Pyroxenite and peridotite xenoliths from Hexigten, Inner Mongolia: Insights into the Paleo-Asian Ocean subduction-related melt/fluid–peridotite interaction. Geochimica Et Cosmochimica Acta, 2014, 140, 435-454.	3.9	40
110	Determination of boron isotope compositions of geological materials by laser ablation MC-ICP-MS using newly designed high sensitivity skimmer and sample cones. Chemical Geology, 2014, 386, 22-30.	3.3	39
111	Structure and composition of the continental crust in East China. Science in China Series D: Earth Sciences, 1999, 42, 129-140.	0.9	37
112	Widespread Neoarchean (~ 2.7–2.6 Ga) magmatism of the Yangtze craton, South China, as revealed by modern river detrital zircons. Gondwana Research, 2017, 42, 1-12.	6.0	36
113	Trace element and <scp>S</scp> r isotope records of multiâ€episode carbonatite metasomatism on the eastern margin of the <scp>N</scp> orth <scp>C</scp> hina <scp>C</scp> raton. Geochemistry, Geophysics, Geosystems, 2017, 18, 220-237.	2.5	35
114	Average chemical compositions of post-Archean sedimentary and volcanic rocks from the Qinling Orogenic Belt and its adjacent North China and Yangtze Cratons. Chemical Geology, 1991, 92, 261-282.	3.3	34
115	Sensitivity improvement in laser ablation inductively coupled plasma mass spectrometry achieved using a methane/argon and methanol/water/argon mixed gas plasma. Analyst, The, 2011, 136, 4925.	3.5	34
116	Poisson's ratio of eclogite: the role of retrogression. Earth and Planetary Science Letters, 2001, 192, 523-531.	4.4	32
117	Results for Rarely Determined Elements in MPIâ€DING, USGS and NIST SRM Glasses Using Laser Ablation ICPâ€MS. Geostandards and Geoanalytical Research, 2009, 33, 319-335.	3.1	32
118	Accurate determination of elements in silicate glass by nanosecond and femtosecond laser ablation ICP-MS at high spatial resolution. Chemical Geology, 2015, 400, 11-23.	3.3	32
119	Geochemistry of early Paleozoic alkali dyke swarms in south Qinling and its geological significance. Science in China Series D: Earth Sciences, 2003, 46, 1292-1306.	0.9	31
120	Pb and Nd isotopic composition of the Jigongshan granite: constraints on crustal structure of Tongbaishan in the middle part of the Qinling–Tongbai–Dabie orogenic belt, Central China. Lithos, 2004, 73, 215-227.	1.4	31
121	Garnet-rich granulite xenoliths from the Hannuoba basalts, North China: Petrogenesis and implications for the Mesozoic crust-mantle interaction. Journal of Earth Science (Wuhan, China), 2010, 21, 669-691.	3.2	31
122	Reassessment of HF/HNO ₃ Decomposition Capability in the High-Pressure Digestion of Felsic Rocks for Multi-Element Determination by ICP-MS. Geostandards and Geoanalytical Research, 2012, , no-no.	3.1	31
123	Simultaneous Determination of Major and Trace Elements in Fused Volcanic Rock Powders Using a Hermetic Vessel Heater and <scp>LA</scp> â€< scp>ICPâ€< scp>MS. Geostandards and Geoanalytical Research, 2013, 37, 207-229.	3.1	31
124	Geochemical and isotopic constraints on the age and origin of mafic dikes from eastern Shandong Province, eastern North China Craton. International Geology Review, 2012, 54, 1389-1400.	2.1	30
125	LA–ICP–MS monazite U–Pb age and trace element constraints on the granulite-facies metamorphism in the Tongbai orogen, central China. Journal of Asian Earth Sciences, 2014, 82, 90-102.	2.3	30
126	Observations of Large Mass-Independent Fractionation Occurring in MC-ICPMS: Implications for Determination of Accurate Isotope Amount Ratios. Analytical Chemistry, 2011, 83, 8999-9004.	6.5	29

#	Article	IF	CITATIONS
127	Pressure-dependent compatibility of iron in garnet: Insights into the origin of ferropicritic melt. Geochimica Et Cosmochimica Acta, 2017, 197, 356-377.	3.9	28
128	The origin and response of zircon in eclogite to metamorphism during the multi-stage evolution of the Huwan Shear Zone, China: Insights from Lu–Hf and U–Pb isotopic and trace element geochemistry. Gondwana Research, 2013, 23, 726-747.	6.0	27
129	Improved Interâ€calibration of Faraday Cup and Ion Counting for <i>In Situ</i> Pb Isotope Measurements Using LAâ€MCâ€ICPâ€MS: Application to the Study of the Origin of the Fangshan Pluton, North China. Geostandards and Geoanalytical Research, 2015, 39, 467-487.	3.1	27
130	Paleo-Asian oceanic subduction-related modification of the lithospheric mantle under the North China Craton: Evidence from peridotite xenoliths in the Datong basalts. Lithos, 2016, 261, 109-127.	1.4	27
131	Microgeochemistry of rutile and zircon in eclogites from the CCSD main hole: Implications for the fluid activity and thermo-history of the UHP metamorphism. Lithos, 2010, 115, 51-64.	1.4	26
132	U–Pb zircon age, geochemical and Sr–Nd isotopic data as constraints on the petrogenesis and emplacement time of the Precambrian mafic dyke swarms in the North China Craton (NCC). Lithos, 2012, 140-141, 38-52.	1.4	26
133	Signal enhancement in laser ablation inductively coupled plasma-mass spectrometry using water and/or ethanol vapor in combination with a shielded torch. Journal of Analytical Atomic Spectrometry, 2014, 29, 536.	3.0	26
134	Geochemistry and U-Pb zircon geochronology of Late-Mesozoic lavas from Xishan, Beijing. Science in China Series D: Earth Sciences, 2006, 49, 50-67.	0.9	25
135	Geochemistry of high-Mg andesites from the early Cretaceous Yixian Formation, western Liaoning: Implications for lower crustal delamination and Sr/Y variations. Science in China Series D: Earth Sciences, 2006, 49, 904-914.	0.9	25
136	Big insights from tiny peridotites: Evidence for persistence of Precambrian lithosphere beneath the eastern North China Craton. Tectonophysics, 2015, 650, 104-112.	2.2	25
137	An Sm-Nd isotopic dating study of the Archean Kongling Complex in the Huangling area of the Yangtze Craton. Science Bulletin, 1998, 43, 1187-1191.	1.7	24
138	Accurate Determination of Rare Earth Elements in USCS, NIST SRM, and MPI-DING Glasses by Excimer LA-ICP-MS at High Spatial Resolution. Spectroscopy Letters, 2008, 41, 228-236.	1.0	24
139	Direct Determination of Tellurium in Geological Samples by Inductively Coupled Plasma Mass Spectrometry Using Ethanol as a Matrix Modifier. Applied Spectroscopy, 2006, 60, 781-785.	2.2	22
140	Comparative Sr–Nd–Hf–Os–Pb isotope systematics of xenolithic peridotites from Yangyuan, North China Craton: Additional evidence for a Paleoproterozoic age. Chemical Geology, 2012, 332-333, 1-14.	3.3	22
141	Geochemical, Sr–Nd isotopic, and zircon U–Pb geochronological constraints on the petrogenesis of Late Paleoproterozoic mafic dykes within the northern North China Craton, Shanxi Province, China. Precambrian Research, 2013, 236, 182-192.	2.7	21
142	Zircon U–Pb age, geochemical, and Sr–Nd–Hf isotopic constraints on the origin of mafic dykes in the Shaanxi Province, North China Craton, China. Lithos, 2013, 175-176, 244-254.	1.4	21
143	Review of High-Precision Sr Isotope Analyses of Low-Sr Geological Samples. Journal of Earth Science (Wuhan, China), 2015, 26, 763-774.	3.2	21
144	An Investigation of Digestion Methods for Trace Elements in Bauxite and Their Determination in Ten Bauxite Reference Materials Using Inductively Coupled Plasmaâ€Mass Spectrometry. Geostandards and Geoanalytical Research, 2016, 40, 195-216.	3.1	21

#	Article	IF	CITATIONS
145	Niobium and Tantalum Concentrations in NIST SRM 610 Revisited. Geostandards and Geoanalytical Research, 2008, 32, 347-360.	3.1	20
146	Triassic high-pressure metamorphism in the Huwan shear zone: Tracking the initial subduction of continental crust in the whole Dabie orogen. Lithos, 2012, 136-139, 60-72.	1.4	20
147	Discovery of dunite and pyroxenite xenoliths in Mesozoic diorite at Jinling, western Shandong and its significance. Science Bulletin, 2003, 48, 1599-1604.	1.7	19
148	Zircon U–Pb age and Sr–Nd–Hf isotopic constraints on the age and origin of Triassic mafic dikes, Dalian area, Northeast China. International Geology Review, 2013, 55, 249-262.	2.1	19
149	Further investigation into ICP-induced elemental fractionation in LA-ICP-MS using a local aerosol extraction strategy. Journal of Analytical Atomic Spectrometry, 2015, 30, 941-949.	3.0	19
150	Direct Determination of Si Isotope Ratios in Natural Waters and Commercial Si Standards by Ion Exclusion Chromatography Multicollector Inductively Coupled Plasma Mass Spectrometry. Analytical Chemistry, 2014, 86, 9301-9308.	6.5	18
151	Geochemistry of the high-Mg andesites at Zhangwu, western Liaoning: Implication for delamination of newly formed lower crust. Science in China Series D: Earth Sciences, 2007, 50, 1773-1786.	0.9	17
152	Zircon U–Pb geochronological, geochemical, and Sr–Nd isotope data for Early Cretaceous mafic dykes in the Tancheng–Lujiang Fault area of the Shandong Province, China: Constraints on the timing of magmatism and magma genesis. Journal of Asian Earth Sciences, 2015, 98, 247-260.	2.3	17
153	Repeated modification of lithospheric mantle in the eastern North China Craton: Constraints from SHRIMP zircon U-Pb dating of dunite xenoliths in western Shandong. Science Bulletin, 2012, 57, 651-659.	1.7	16
154	Multiple exsolutions in a rare clinopyroxene megacryst from the Hannuoba basalt, North China: Implications for subducted slab-related crustal thickening and recycling. Lithos, 2013, 177, 136-147.	1.4	16
155	The Role of Earth's Deep Volatile Cycling in the Generation of Intracontinental Highâ€Mg Andesites: Implication for Lithospheric Thinning Beneath the North China Craton. Journal of Geophysical Research: Solid Earth, 2019, 124, 1305-1323.	3.4	16
156	Sr–Nd isotopic and geochemical constraints on provenance of late Paleozoic to early cretaceous sedimentary rocks in the Western Hills of Beijing, North China: Implications for the uplift of the northern North China Craton. Sedimentary Geology, 2012, 245-246, 17-28.	2.1	15
157	Mesozoic high-Mg andesites from the Daohugou area, Inner Mongolia: Upper-crustal fractional crystallization of parental melt derived from metasomatized lithospheric mantle wedge. Lithos, 2018, 302-303, 535-548.	1.4	14
158	Direct Determination of Ag in Geological Samples by Membrane Desolvation-Inductively Coupled Plasma-Mass Spectrometer. Chinese Journal of Analytical Chemistry, 2008, 36, 1493-1498.	1.7	13
159	K-Ar Ages and Geochemical + Sr-Nd Isotopic Compositions of Adakitic Volcanic Rocks, Western Shandong Province, Eastern China: Foundering of the Lower Continental Crust. International Geology Review, 2008, 50, 763-779.	2.1	13
160	Two-Stage Exhumation of Ultrahigh-Pressure Metamorphic Rocks from the Western Dabie Orogen, Central China. Journal of Geology, 2011, 119, 15-31.	1.4	13
161	U–Pb zircon ages, geochemical and Sr–Nd–Pb isotopic constraints on the dating and origin of intrusive complexes in the Sulu orogen, eastern China. International Geology Review, 2011, 53, 61-83.	2.1	13
162	Geophysical properties of the lower crustal granulites from the Qinling Orogenic Belt, China. Tectonophysics, 1992, 204, 401-408.	2.2	12

#	Article	IF	CITATIONS
163	Improved performance of a shielded torch using ethanol in inductively coupled plasma–sector field mass spectrometry. Spectrochimica Acta, Part B: Atomic Spectroscopy, 2015, 106, 36-44.	2.9	12
164	Variation of molybdenum isotopes in molybdenite from porphyry and vein Mo deposits in the Gangdese metallogenic belt, Tibetan plateau and its implications. Mineralium Deposita, 2016, 51, 201-210.	4.1	12
165	Ablation Characteristic of Ilmenite using <scp>UV</scp> Nanosecond and Femtosecond Lasers: Implications for Nonâ€Matrixâ€Matched Quantification. Geostandards and Geoanalytical Research, 2016, 40, 477-491.	3.1	11
166	Direct Quantitative Determination of Trace Elements in Fineâ€Grained Whole Rocks by Laser Ablationâ€Inductively Coupled Plasmaâ€Mass Spectrometry. Geostandards and Geoanalytical Research, 2011, 35, 7-22.	3.1	10
167	Step-like growth of the continental crust in South China: evidence from detrital zircons in Yangtze River sediments. Lithos, 2018, 320-321, 155-171.	1.4	10
168	Titanite evidence for Triassic thickened lower crust along southeastern margin of North China Craton. Lithos, 2014, 206-207, 277-288.	1.4	9
169	Nb/Ta variations of mafic volcanics on the Archean-Proterozoic boundary: Implications for the Nb/Ta imbalance. Science in China Series D: Earth Sciences, 2005, 48, 1106.	0.9	8
170	Geochemistry of Dabeigou Basalt in Chengde Basin, Hebei Province and Constraints on Lithospheric Mantle Thinning of North China Craton. Earth Science Frontiers, 2007, 14, 98-108.	0.6	8
171	A preliminary study of isopropyl alcohol matrix effect and correction in ICP-MS. Chinese Chemical Letters, 2007, 18, 1297-1300.	9.0	8
172	Petrogenetic significance of high Fe/Mn ratios of the Cenozoic basalts from eastern China. Science in China Series D: Earth Sciences, 2008, 51, 229-239.	0.9	8
173	Reply to the comment by Zhang et al. on: "First finding of A-type and adakitic magmatism association in Songpan–Garze fold belt, eastern Tibetan Plateau: Implication for lithospheric delamination― Lithos, 2008, 103, 565-568.	1.4	8
174	Modification of the lithospheric mantle by melt derived from recycled continental crust evidenced by wehrlite xenoliths in Early Cretaceous high-Mg diorites from western Shandong, China. Science China Earth Sciences, 2012, 55, 1972-1986.	5.2	8
175	Determination of Primary Magnetic Minerals of a Weathered Metapelite Xenolith from Zhouba Region, North China, by Combining Thermomagnetic Runs and Low-Temperature Measurements. Chinese Journal of Geophysics, 2005, 48, 946-952.	0.2	7
176	Magnetic study of mafic granulite xenoliths from the Hannuoba basalt, north China. Geochemistry, Geophysics, Geosystems, 2008, 9, .	2.5	7
177	Episodic Mesozoic thickening and reworking of the North China Archean lower crust correlated to the fast-spreading Pacific plate. Journal of Asian Earth Sciences, 2014, 80, 63-74.	2.3	7
178	Ce anomaly in minerals of eclogite and garnet pyroxenite from Dabie-Sulu ultrahigh pressure metamorphic belt: Tacking subducted sediment formed under oxidizing conditions. Science in China Series D: Earth Sciences, 2004, 47, 920-930.	0.9	6
179	Zircon U-Pb ages of olivine pyroxenite xenolith from Hannuoba: Links between the 97–158 Ma basaltic underplating and granulite-facies metamorphism. Science Bulletin, 2004, 49, 1055-1062.	1.7	6
180	Geochemical, Sr–Nd–Pb isotope, and zircon U–Pb geochronological constraints on the origin of Early Permian mafic dikes, northern North China Craton. International Geology Review, 2013, 55, 1626-1640.	2.1	6

#	Article	IF	CITATIONS
181	Garnet–spinel–corundum–quartz-bearing titanohematite veins in eclogite from the Sulu ultrahigh-pressure terrane: Imprint of a short-lived, high-temperature metamorphic stage. Journal of Asian Earth Sciences, 2011, 42, 704-714.	2.3	5
182	Poisson's ratio of eclogite: Implications for lower crustal delamination of orogens. Science in China Series D: Earth Sciences, 2003, 46, 909-918.	0.9	4
183	Age and origin of a Palaeozoic nepheline syenite from northern Shanxi Province, China: U–Pb zircon age and whole-rock geochemical and Sr–Nd isotopic constraints. International Geology Review, 2012, 54, 1296-1308.	2.1	3
184	Application of an Orthogonal Method for Optimizing an Inductively Coupled Plasma Mass Spectrometer Analytical Sciences, 2002, 18, 701-704.	1.6	2
185	The rise of atomic spectrometry in China over the past 25 years. Journal of Analytical Atomic Spectrometry, 2010, 25, 1803.	3.0	1